





Deep Recurrent Neural Network with Tanimoto Similarity and MKSIFT Features for Medical Image Search and Retrieval

Hardik H. Bhatt¹(✉)  and Anand P. Mankodia² 

¹ Research Scholar, Ganpat University, Gujarat, India
hbhatt992@gmail.com

² Department of Electronics and Communication, Ganpat University, Gujarat, India

Abstract. The innovation of digital medical images has led to the requirement of rich descriptors and efficient retrieval tool. Thus, the Content Based Image Retrieval (CBIR) technique is essential in the domain of image retrieval. Due to the growing medical image data, the searching or retrieving a relevant image from the dataset is a major problem. To address this problem, this paper propose a new medical image retrieval technique, namely Multiple Kernel Scale Invariant Feature Transform-based Deep Recurrent Neural Network (MKSIFT-Deep RNN) using the image contents. The goal is to present an effective tool that can be utilized for effective retrieval of image from huge medical image database. Here, MKSIFT is adapted for extracting the relevant features obtained from acquired input image. Moreover, MKSIFT evaluates the key point descriptor using kernels functions, wherein the weights are allocated to kernels. The feature vectors are employed in the Deep RNN for classifying the images by training the classifier, which is considered as training phase. In testing phase, a set of query images is given to the classifier which adapts Tanimoto similarity for retrieving the images. The proposed MKSIFT-Deep RNN outperformed other methods with maximal precision of 93.723%, maximal recall of 93.652% and maximal F-measure of 93.687%.

Keywords: Computer vision · Medical images · Multiple Kernel Scale Invariant Feature Transform (MKSIFT) · Deep recurrent neural network · Image retrieval

1 Introduction

The information retrieval is a trending domain due to medical imaging systems as it deal with audio, image and video which provide huge information that changes the world of medicines. In recent times, the huge-scaled medical image search acquired more consideration in the retrieval of images from big sized image datasets [5]. The innovation in medical imaging technologies increased due to the use of Internet, digital cameras, and smart-phone. The stored medical image data are increasing and for searching and retrieving the relevant medical image from an archive is challenging issue. The need of any medical image retrieval model is to assemble and search the medical images that are

visual semantic relation using the query provided by the user [6]. There is also a need to search images from the dataset which is handled by model for effectual recovery of medical images [7].

The CBIR is adapted on existing techniques and gained interest in the retrieval of medical images. Different feature extraction methods are adapted on the basis of boundary contour, spatial layout, color, and texture. In [8], CBIR technique is devised using the features like histograms of oriented gradients (HOG), SIFT, and local binary pattern (LBP), for attaining improved results in image retrieval. In [9], improved CBIR technique is developed using certain attributes like wavelet-based histogram approaches that utilize relevance feedback for retrieving the images. An optimized technique is devised in [10] for pattern retrieval on the basis of quantized histograms. In [11], a technique is devised for training deep convolutional neural network (DCNN) in order to enhance the CBIR.

This research presents a novel method, namely MKSIFT-Deep RNN for medical image retrieval using data set of medical images. Here, MKSIFT feature is adapted for generating the feature vector by extracting significant features from the medical image database. The purpose is to retrieve the images from the huge database. Here, MKSIFT is adapted for extracting the relevant features using acquired input image. Moreover, MKSIFT evaluates the key point descriptor using kernel function, wherein the weights are allocated to the kernels. The feature vectors are employed in the Deep RNN for classifying the images by training the classifier, which is considered as training phase. In testing phase, a set of query images is given to the classifier which adapts Tanimoto similarity for retrieving the images.

The major contribution of the research is:

- **Proposed MKSIFT-Deep RNN for Medical Image Retrieval:** Develop a novel medical image retrieval model, namely Multiple Kernel Scale Invariant Feature Transform-based deep recurrent neural network (MKSIFT-Deep RNN) for effective medical image retrieval.

2 Motivation

From the literary works, the CBIR models are devised and modified using deep learning approaches. However, there are still some issues which are not addressed. Firstly, the semantic gap is unsolved that still exist between low level feature representation of medical images. Moreover, the issues confronted by the existing methods stood as the motivation for devising a novel medical image retrieval method.

2.1 Literature Review

The eight existing techniques based on medical image retrieval is deliberated below: Mathan Kumar, B. and Pushpa Lakshmi, R [1] devised a method for effective retrieval of image. Here, MKSIFT was adapted for extracting the features from the pre-processed image. The MKSIFT computed key point descriptor with kernel functions for selecting the weights using Particle Swarm-Fractional Bacterial foraging optimization (PS-FBFO). The method adapted cross-indexed image search by transforming the feature

points to binary codes. However, the method failed to use advanced optimization techniques like lion optimization for choosing the weight coefficients to enhance performance. Sharif, U *et al.* [2] developed a technique by hybridizing visual words with SIFT. The local feature descriptors were selected that adds harmonizing upgrading to CBIR. The SIFT descriptor was able to detect the objects vigorously under cluttering because of rotation, noise, and illumination variance. The method enhanced the performance of CBIR, but failed to use deep learning model for huge scale Image Retrieval. Saritha, R.R. *et al.* [3] developed deep belief network (DBN) technique for CBIR. The method extracted the features and the classification was initiated using DBN for classifying the images. The DBN was trained using effective feature representations for retrieving the relevant images. However, the method failed to provide real time feature extraction. Xia, Z *et al.* [4] devised an outsourced CBIR method using bag-of-encrypted-words (BOEW) model for retrieving images. Here, the method utilized permutation, and color value substitution. Moreover, the BOEW model was designed for representing each image using feature vector. The similarity between the images was computed using Manhattan distance. However, the method failed to utilize local descriptors for BOEW model.

2.2 Challenges

The challenges confronted by the existing methodologies are deliberated below:

- Even though, different methods are devised for medical image retrieval [20] semantic gap remains a challenging issue in current CBIR methods. The semantic gap exist-samid low-level image pixels obtained via machine and high-level semantic concept obtained via humans [3].
- In [1], outsourced CBIR scheme is devised using bag-of-encrypted-words (BOEW) model for retrieving the images from massive datasets. The method is effective for faster retrieval, but confronted issues like complex computations and heavy storage.
- The proficient recovery of images using massive image datasets is major issue. In recent days, the images are retrieved using visual information and CBIT techniques.

3 Proposed MK-SIFT-Based Deep RNN for Image Retrieval

Figure 1 illustrates the schematic view of medical image retrieval model using proposed MK-SIFT-based Deep-RNN. Initially, the medical images are fed to feature extraction module. The extraction of features is done using MK-SIFT [1]. Once the significant features are obtained, then the group retrieval is performed using the generated features and Deep RNN [12]. The training of Deep RNN is performed using the MKSIFT features for tuning the optimal weights in order to perform group retrieval. Here, query image is given as an input, which is further matched with the classified images using Tanimoto similarity measure [13]. Thus, the image retrieval is performed using Tanimoto similarity measure. By computing the similarity between query image and classified image set using Tanimoto similarity measure, the retrieval of relevant instances is done. The briefer illustration of each steps is illustrated in the below section.

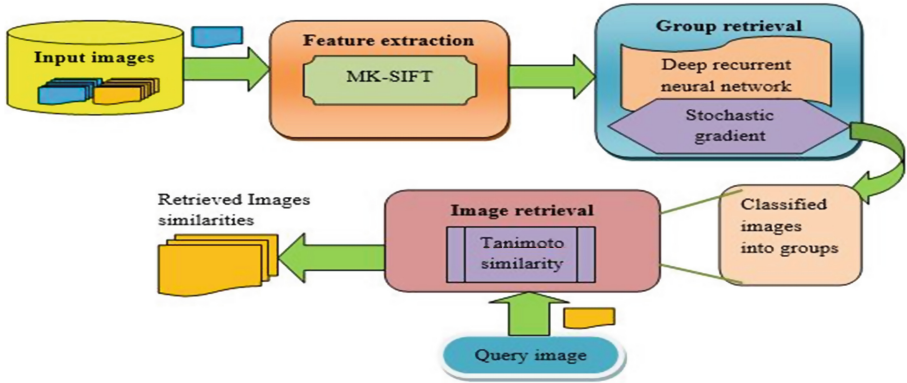


Fig. 1. Schematic view of CBIR using proposed MK-SIFT-based Deep RNN

Assume a database D with d number of medical images and is represented as,

$$D = \{I_1, I_2, \dots, I_k, \dots, I_l\} \quad (1)$$

where, I_k represent k^{th} input image, and l indicate total number of images.

Each image I_k is processed for extracting the significant features using MKSIFT approach which is elaborated in the below subsection.

3.1 Extraction of Significant Feature Using MK-SIFT

The noteworthy features obtained from input image and the connotation of feature extraction is to produce highly relevant features which facilitate improved retrieval of medical images. Meanwhile, the complexity of analyzing the medical image is reduced as the image is modelled as the reduced set of features. In addition, the precision allied with the classification is guaranteed with efficient feature extraction for which the MKSIFT [1] approach is employed. The MKSIFT is a feature extraction technique which is devised by modifying the SIFT feature with different weightage method in key point descriptor for extracting features from input medical image. The MKSIFT-based feature extraction is classified into different steps which involve extremadetection, key point's removal, assignment of orientation, and calculation of descriptors. Moreover, the Gaussian function present in the key point descriptor is restored with exponential kernel and tangential kernel functions.

SIFT [14] is a method which transforms the image into different scale invariants on the basis of local features. The method devises vast features which covers the complete variety of images. For matching images, the SIFT features are mined from images. The four steps considered for the generating the feature set which are described below:

(i) Discovery of Scale-Space Extrema: The first phase for extracting feature is to determine the location and image scales by detecting steady features over scales considering Gaussian function, that can be modelled as,

$$S(m, n, \alpha) = G(m, n, \alpha) * I(m, n) \quad (2)$$

Where, $I(m, n)$ represent input medical image, $*$ indicate convolution operator, $G(m, n, \alpha)$ denote Gaussian function.

The Gaussian function is expressed as,

$$G(m, n, \alpha) = \frac{1}{2\pi\alpha^2} e^{-(m^2+n^2)/2\alpha^2} \quad (3)$$

In [15], scale-space extrema is employed in difference-of-Gaussian (DoG) function to determine key point localization. This is represented by a function, $X(m, n, \alpha)$ generated by the difference between two scales, which are detached by a constant as,

$$X(m, n, \alpha) = G(m, n, v\alpha) - G(m, n, \alpha) \quad (4)$$

$$X(m, n, \alpha) = S(m, n, v\alpha) - S(m, n, \alpha) \quad (5)$$

where, v indicate constant.

In addition, the DoG function provides an approximation based on the Laplacian of Gaussian $\alpha^2 \nabla^2 G$. From the equation, the relation between $\alpha^2 \nabla^2 G$ is,

$$\frac{\partial G}{\partial \alpha} = \alpha^2 \nabla^2 G \quad (6)$$

The extrema are determined using each sample point, which is further compared to its neighbours and other nine neighbours that reside in scale. The point is chosen if result is either larger or smaller.

(ii) Localization of Key Point: After detecting key points, the subsequent steps are followed which is elimination of key points with low contrast by carrying a data fit for determining the scale and location. This is computed on the basis of expansion of scale-space function using Taylor series by,

$$X(g) = X + \frac{\partial X}{\partial g} g + \frac{1}{2} g^T \frac{\partial^2 X}{\partial g^2} g \quad (7)$$

where, g indicate offset given by $g = (m, n, \alpha)^T$

The location is expressed as,

$$g = -\frac{\partial^2 X^{-1} \partial X}{\partial g^2 \partial g} \quad (8)$$

While the offset is instituted to be larger than value of threshold, then the extremum is at the diverse sample point, which holds low contrast. Hence, by this assessment, the low contrast key point is eliminated. The unstable extrema with low contrast are eliminated using function $K(\hat{d})$ expressed as:

$$X(\hat{g}) = X + \frac{1}{2} \frac{\partial X^T}{\partial g} \hat{g} \quad (9)$$

In DoG, an anomalous peak poses a outsized principal curvature, which is removed. The principal curvatures isevaluated considering Hessian matrix as,

$$K = \begin{bmatrix} X_{mm} & X_{mn} \\ X_{mn} & X_{nn} \end{bmatrix} \quad (10)$$

where, K represent Hessian matrix.

(iii) Assignment of Orientation: The key point descriptor is expressed using proper orientation assignment considering key points based on local images. For evaluating the scale invariant, the Gaussian smoothed image is chosen considering scale of the key point. The magnitude and orientation is computed using pixel differences as follows:

$$M(m, n) = \sqrt{(S(m+1, n) - S(m-1, n))^2 + (S(m, n+1))^2} \quad (11)$$

$$\varphi(m, n) = \tan^{-1}((S(m, n+1) - M(m, n-1))/((m(m+1, n) - M(m-1, n))) \quad (12)$$

where $M(m, n)$ indicate magnitude, $w(m, n)$ represent orientation, and S indicate scale space. Based on magnitude and orientations of the key point, a histogram based on the orientation is designed.

(iv) Computation of Descriptor Using Multi-kernel Function: The last phase is computation of key point descriptor using image gradients considering region of key point. On the basis of scale of key point, the orientation and the magnitude are computed to choose the Gaussian blur level of image. The coordinate of descriptor are rotated on the basis of orientation of key point to determine the orientation invariance. However, Gaussian function could not protect image brightness, offering less emphasis to gradients. Thus, MKSIFT method devises two kernel functions, namely tangential and exponential kernels which help to augment variance, thereby minimizing relics of image. Thus, the weight function of MKSIFT is expressed as,

$$W = M(m, n) * w(m, n) \quad (13)$$

The kernel function is represented by,

$$w(m, n) = \eta * \exp(f(m, n)) + \rho * \tanh f(m, n) \quad (14)$$

where, η and ρ represent weight coefficients that ranges between $[0, 1]$.

The obtained features is accumulated in the feature vector denoted as F ; ($1 \leq a \leq e$). The feature vector F is fed to the Deep RNN for classifying the images into groups.

3.2 Classifying the Medical Images for Group Retrieval Using Deep RNN

The Deep RNN is employed to retrieve the groups considering the MKSIFT features. The architecture of Deep RNN is portrayed below.

3.2.1 Architecture of Deep RNN

The features F extracted from the input images are given as the input to the Deep RNN classifier. Deep RNN [12] is the network architecture that contains multiple recurrent hidden layers in network hierarchy layer. In Deep RNN the recurrent connection exists at the hidden layer. The Deep RNN classifier operates effectively under the varying input feature length based on the sequence of information. It uses the knowledge of previous state as input in the current prediction and process the iteration using the hidden state information. The recurrent feature makes the Deep RNN to be highly effective in working with the features. Due to the sequential pattern of information, Deep RNN is considered as the best classifier among traditional deep learning approaches. The architecture of Deep RNN is represented in Fig. 2.

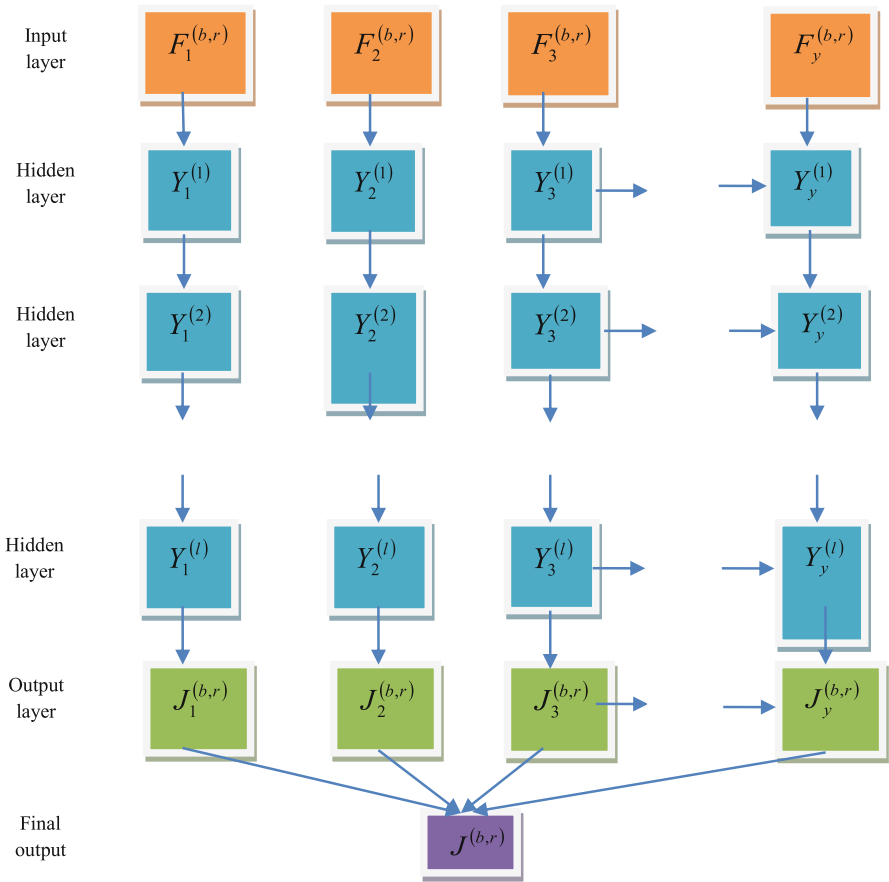


Fig. 2. Architecture of Deep RNN classifier

The structure of Deep RNN is made by considering the input vector of b^{th} layer at r^{th} time as $F^{(b,r)} = \{F_1^{(b,r)}, F_2^{(b,r)}, \dots, F_i^{(b,r)}, \dots, F_y^{(b,r)}\}$ and the output vector of b^{th}

layer at r^{th} time as, $J^{(b,r)} = \{J_1^{(b,r)}, J_2^{(b,r)}, \dots, J_i^{(b,r)}, \dots, J_y^{(b,r)}\}$, respectively. The pair of each elements of input and the output vectors is termed as the unit. Here, i denotes the arbitrary unit number of b^{th} layer, and y represents the total number of units of b^{th} layer. In addition to this, the arbitrary unit number and the total number of units of $(b-1)^{th}$ layer is denoted as j and E , respectively. At this time, the input propagation weight from $(b-1)^{th}$ layer to b^{th} layer is expressed as, $W^{(b)} \in H^{y \times E}$, and the recurrent weight of b^{th} layer is modelled as $w^{(b)} \in H^{y \times y}$. Here, H denotes the set of weights. However, the components of the input vector is expressed as,

$$F_i^{(b,r)} = \sum_{z=1}^E p_{iz}^{(b)} J_z^{(b-1,r)} + \sum_{i'}^y x_{ii'}^{(b)} J_{i'}^{(b,r-1)} \quad (15)$$

where, $p_{iz}^{(b)}$ and $x_{ii'}^{(b)}$ are the elements of $W^{(b)}$ and $w^{(b)}$. i' denotes the arbitrary unit number of b^{th} layer. The elements of the output vector of b^{th} layer is represented as,

$$J_i^{(b,r)} = \beta^{(b)} \left(F_i^{(b,r)} \right) \quad (16)$$

where, $\beta^{(b)}$ denotes the activation function. However, the activation functions, like sigmoid function as $\beta(F) = \tanh(F)$, rectified linear unit function (ReLU) as $\beta(F) = \max(F, 0)$, and the logistic sigmoid function as $\beta(F) = \frac{1}{(1+e^{-F})}$ are the frequently used activation function.

To simplify the process, 0^{th} weight as $p_{i0}^{(b)}$ and 0^{th} unit as $J_0^{(b-1,r)}$ are introduced and hence the bias is represented as,

$$J^{(b,r)} = \beta^{(b)} \cdot \left(W^{(b)} J^{(b-1,r)} + w^{(b)} \cdot J^{(b,r-1)} \right) \quad (17)$$

Here, $J^{(b,r)}$ denotes the output of classifier.

3.3 Image Retrieval Using Tanimoto Measure Based Similarity

For effective image retrieval, a query image Q is fed to the feature extractor and is described for producing its new feature vector F' ; ($1 \leq a \leq e$). The searching is done by matching training feature vector F against new feature F' using Tanimoto similarity measure. The feature fetches the matching images as the result of search output. The Tanimoto metric is represented as,

$$\frac{\sum_{a=1}^e h_a c_a}{\sum_{a=1}^e h_a^2 + \sum_{a=1}^e c_a^2 - \sum_{a=1}^e h_a c_a} \quad (18)$$

where, h_a represent a^{th} feature residing in feature vector F , and c_a indicate the a^{th} feature residing in feature vector F' .

Thus, the Tanimoto similarity is employed for retrieving the relevant images from the classified database.

4 Results and Discussion

This comparison of proposed method with conventional methods using precision, F-measure and recall is illustrated. In addition, the effectiveness of proposed MKSIFT-Deep RNN method is analyzed by varying number of query.

4.1 Experimental Setup

The execution of proposed MKSIFT-Deep RNN is done in PYTHON using PC having Windows 10 OS, 4 GB RAM, and Intel i5 core processor.

4.2 Dataset Description

The medical image dataset employed for the experimentation to describe the analysis of performance using each medical image retrieval method is described below. Here, the database is designed by considering prostate cancer images, retinal images, iris images, breast cancer images, skin cancer images, bacilli images, and BRATS dataset images [17–19].

4.3 Evaluation Metrics

The effectiveness of proposed MKSIFT-Deep RNN is employed for analyzing methods includes the precision, recall and F-measure.

4.3.1 Precision

The precision parameter defines the ratio of relevant images from the retrieved images considering a query and is given as,

$$precision = \frac{|rel \cap ret|}{|ret|} \quad (19)$$

where, *rel* denote relevant images, *ret* represent retrieved images.

4.3.2 Recall

The ratio of total relevant images that are actually retrieved is given as,

$$recall = \frac{|rel \cap ret|}{|rel|} \quad (20)$$

4.3.3 F-measure

The harmonic mean of recall and precision is termed as F-measure and is represented as,

$$F - measure = 2 * \frac{precision * recall}{precision + recall} \quad (21)$$

4.4 Comparative Methods

The methods employed for the analysis include: SIFT [14], HOG + MKSIFT (Applied HOG [16] in MKSIFT), MKSIFT [1], and proposed MKSIFT-Deep RNN algorithm.

4.4.1 Analysis Based on Query Set-1

Figure 3 portrays the analysis of methods considering query set-1 using precision, recall and F-measure parameter. Each query set poses 15 images from the acquired database. The analysis based on precision parameter is described in Fig. 3a. When the number of query is 4, the precision values computed by SIFT, HOG + MKSIFT, MKSIFT, and proposed MKSIFT-Deep RNN are 85.706%, 89.043%, 89.584%, and 90.124%. Likewise, when the number of query is 18, the precision values computed by SIFT, HOG + MKSIFT, MKSIFT, and proposed MKSIFT-Deep RNN are 91.384%, 92.103%, 93.183%, and 93.723%. The analysis based on recall parameter is portrayed in Fig. 3b. When the number of query is 4, the recall values computed by SIFT, HOG + MKSIFT, MKSIFT, and proposed MKSIFT-Deep RNN are 75.884%, 77.246, 77.446, and 83.693%. Similarly, when the number of query is 18, the recall values computed by SIFT, HOG + MKSIFT, MKSIFT, and proposed MKSIFT-Deep RNN are 78.301%, 80.859%, 81.159%, and 86.415%. The analysis based on F-measure parameter is portrayed in Fig. 3c. When the number of query is 4, the recall values computed by SIFT,

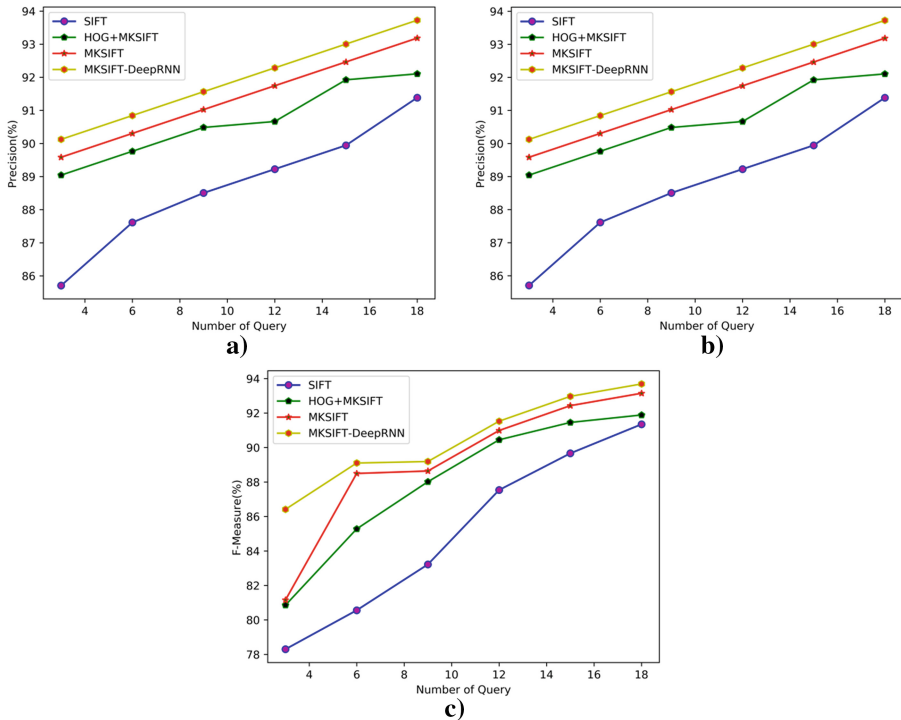


Fig. 3. Analysis based on query set-1 considering a) Precision b) Recall c) F-measure

HOG + MKSIFT, MKSIFT, and proposed MKSIFT-Deep RNN are 91.347%, 91.887%, 93.147%, and 93.687%. Similarly, when the number of query is 18, the recall values computed by SIFT, HOG + MKSIFT, MKSIFT, and proposed MKSIFT-Deep RNN are 91.42%, 91.959%, 93.219% and 93.76%.

4.4.2 Analysis Based on Query Set-2

Figure 4 portrays the analysis of methods considering query set-2 using precision, F-measure and recall parameter. The analysis using precision parameter is described in Fig. 3a. When the number of query is 4, the precision values computed by SIFT, HOG + MKSIFT, MKSIFT, and proposed MKSIFT-Deep RNN are 85.785%, 88.989%, 89.53%, and 90.07%. Likewise, when the number of query is 18, the precision values computed by SIFT, HOG + MKSIFT, MKSIFT, and proposed MKSIFT-Deep RNN are 92.049%, 92.589%, 93.129%, and 93.67%. The analysis based on recall parameter is portrayed in Fig. 4b. When the number of query is 4, the recall values computed by SIFT, HOG + MKSIFT, MKSIFT, and proposed MKSIFT-Deep RNN are 79.711%, 82.266%, 84.046%, and 84.396%. Similarly, when the number of query is 18, the recall values computed by SIFT, HOG + MKSIFT, MKSIFT, and proposed MKSIFT-Deep RNN are 92.031%, 92.572%, 93.111%, and 93.652%. The analysis based on F-measure parameter is portrayed in Fig. 4c. When the number of query is 4, the recall values computed

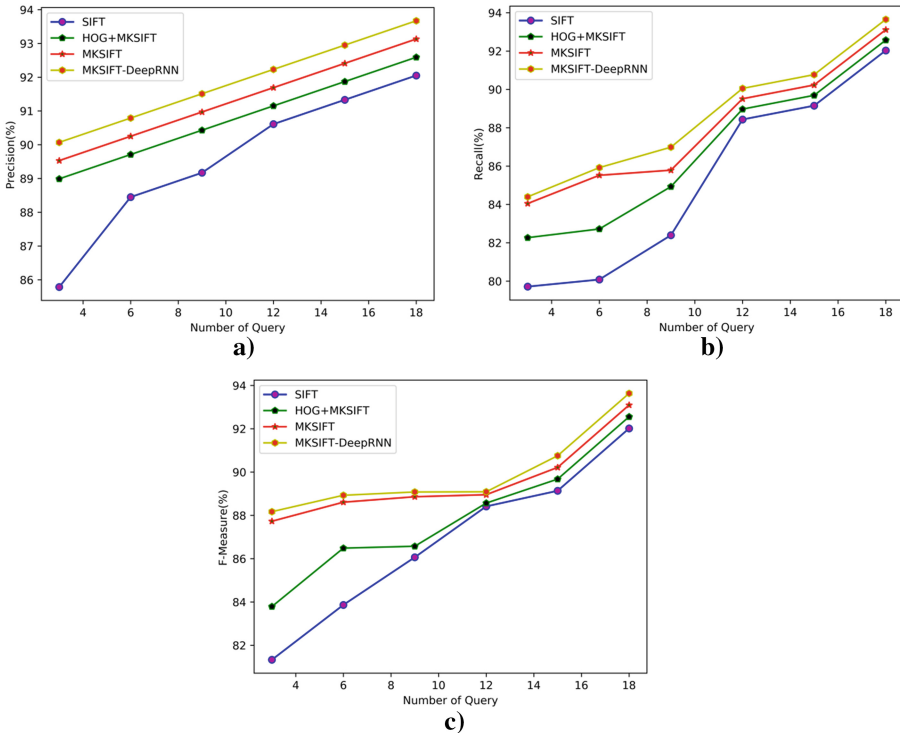


Fig. 4. Analysis based on query set-2 considering a) Precision b) Recall c) F-measure

by SIFT, HOG + MKSIFT, MKSIFT, and proposed MKSIFT-Deep RNN are 81.329%, 83.787%, 87.728%, and 88.170%. Similarly, when the number of query is 18, the recall values computed by SIFT, HOG + MKSIFT, MKSIFT, and proposed MKSIFT-Deep RNN are 92.013%, 92.553%, 93.093%, and 93.634%.

5 Conclusion

This research proposes an image retrieval model, namely MKSIFT-Deep RNN for retrieving the relevant image from the medical image database. Here, MKSIFT approach is employed for selecting the relevant feature from the database. The MKSIFT utilizes the SIFT wherein key point descriptor is computed based on different kernel functions. In MKSIFT, the weight is assumed to be stable for classifying the input images. In addition, Deep RNN is employed for classifying the images into groups using generated feature vector. Whenever the query set is given to the proposed MKSIFT-Deep RNN, the medical image is processed to extract the features in order to devise the image contents. These features adapt Tanimoto similarity measure for comparing the images of the classified database for effective image retrieval. The proposed MKSIFT-Deep RNN outperformed other methods with maximal precision of 93.723%, maximal recall of 93.652% and maximal F-measure of 93.687%. For future works, some advanced optimization techniques can be employed to train the deep classifier in order to improve performance by accomplishing better image retrieval.

References

1. Mathan Kumar, B., Pushpa Lakshmi, R.: Multiple kernel scale invariant feature transform and cross indexing for image search and retrieval. *Imaging Sci. J.* **66**(2), 84–97 (2018)
2. Sharif, U., Mehmood, Z., Mahmood, T., Javid, M.A., Rehman, A., Saba, T.: Scene analysis and search using local features and support vector machine for effective content-based image retrieval. *Artif. Intell. Rev.* **52**(2), 901–925 (2018). <https://doi.org/10.1007/s10462-018-9636-0>
3. Saritha, R.R., Paul, V., Kumar, P.G.: Content based image retrieval using deep learning process. *Cluster Computing* **22**(2), 4187–4200 (2018). <https://doi.org/10.1007/s10586-018-1731-0>
4. Xia, Z., Jiang, L., Liu, D., Lu, L. and Jeon, B., “BOEW: A content-based image retrieval scheme using bag-of-encrypted-words in cloud computing,” *IEEE Transactions on Services Computing*, 2019
5. Zhou, W., Li, H., Hong, R., et al.: BSIFT: toward data-independent codebook for large scale image search. *IEEE Trans. Image Process.* **24**(3), 967–979 (2015)
6. Latif, A., et al.: Content-based image retrieval and feature extraction: a comprehensive review. *Math. Problems Eng.* (2019)
7. Munjal, M.N. and Bhatia, S.: A novel technique for effective image gallery search using content based image retrieval system. In: *Proceedings of International Conference on Machine Learning, Big Data, Cloud and Parallel Computing*, pp. 25–29. IEEE (2019)
8. Yu, J., Qin, Z., Wan, T., Zhang, X.: Feature integration analysis of bag-of-features model for image retrieval. *Neuro Comput.* **120**, 355–364 (2013)
9. Raja, N.M.K., Bhanu, K.S.: Content bases image search and retrieval using indexing by k means clustering technique. *Int. J. Adv. Res. Comput. Commun. Eng.* **2**(5), 2181–2189 (2013)

10. Zhong, D., Defée, I.: DCT histogram optimization for image database retrieval. *Pattern Recogn. Lett.* **26**(14), 2272–2281 (2005)
11. Tzelepi, M., Tefas, A.: Deep convolutional learning for content based image retrieval. *Neurocomputing* **275**, 2467–2478 (2018)
12. Inoue, M., Inoue, S., Nishida, T.: Deep recurrent neural network for mobile human activity recognition with high throughput. *Artif. Life Robot.* **23**(2), 173–185 (2017). <https://doi.org/10.1007/s10015-017-0422-x>
13. Sergyan, S.: Color histogram features based image classification in content-based image retrieval systems. In: *Proceedings of 6th International Symposium on Applied Machine Intelligence and Informatics*, pp. 221–224 (2008)
14. Lowe, D.G.: Distinctive image features from scale-invariant keypoints. *Int. J. Comput. Vis.* **60**(2), 91–110 (2004)
15. Lowe, D.G.: Object recognition from local scale-invariant features. In: *Proceedings of the Seventh IEEE International Conference on Computer Vision, Kerkyra*, vol. 2, pp. 1150–1157 (1999)
16. Vijendran, A.S., Kumar, S.V.: A new content based image retrieval system by HOG of wavelet sub bands. *Int. J. Sig. Process. Image Process. Pattern Recogn.* **8**(4), 297–306 (2015)
17. Menze, B.H., Jakab, A., Bauer, S., Kalpathy-Cramer, J., Farahani, K., Kirby, J., et al.: The multimodal brain tumor image segmentation benchmark (BRATS). *IEEE Trans. Med. Imaging* **34**(10), 1993–2024 (2015). <https://doi.org/10.1109/TMI.2014.2377694>
18. Bakas, S., Akbari, H., Sotiras, A., Bilello, M., Rozycki, M., Kirby, J.S., et al.: Advancing The Cancer Genome Atlas glioma MRI collections with expert segmentation labels and radiomic features. *Nat. Sci. Data* **4**, 170117 (2017). <https://doi.org/10.1038/sdata.2017.117>
19. S. Bakas, et al.: Identifying the best machine learning algorithms for brain tumor segmentation, progression assessment, and overall survival prediction in the BRATS challenge. *arXiv preprint arXiv:1811.02629* (2018)
20. Chaubey, N.K., Jayanthi, P.: Disease diagnosis and treatment using deep learning algorithms for the healthcare system. In: Wason, R., Goyal, D., Jain, V., Balamurugan, S., Baliyan, A. (eds.), *Applications of Deep Learning and Big IoT on Personalized Healthcare Services*, pp. 99–114. IGI Global, Hershey (2020). <https://doi.org/10.4018/978-1-7998-2101-4.ch007>